ACS OMEGA

Open Access

http://pubs.acs.org/journal/acsodf

Article

Experimental Study on Carbon Dioxide Displacement by Coal Seam Water Injection

Tianwei Shi, Yishan Pan, Aiwen Wang,* Lianpeng Dai, and Helian Shen*

Cite This: *ACS Omega* 2024, 9, 14075−14083

Read Online

ACCESS | Metrics & More | Article Recommendations

ABSTRACT: Using water to displace carbon dioxide adsorbed in coal can prevent coal and gas outbursts. However, the mechanism of continuous water injection replacing adsorbed gases in coal has not been well studied. An experiment with the same water injection pressure and different adsorption equilibrium pressures for displacing carbon dioxide was conducted. The variation patterns of the amount of displaced carbon dioxide, time, and water displacement rate, displacement ratio, and water action ratio were analyzed. The modes of water injection displacing carbon dioxide are discussed. The results show that the change in the amount of displaced carbon dioxide consists of three stages: rapid, slow, and stop growth stages. For the same displacement time, as the adsorption equilibrium pressure rises, more carbon dioxide is displaced. The time displacement rate and water displacement rate can be divided into three stages: rising, peak, and dropping stages. As the adsorption equilibrium pressure increases, the duration of the peak stage decreases, while the time and water displacement rates increase. At different adsorption equilibrium pressures, the carbon dioxide displacement ratio ranged from 45% to 54%, less than the natural desorption ratio. But the water action ratio containing the gas dissolution amount was close to or greater than the natural desorption ratio. Thus, the displacement effect of flowing water accelerated the desorption of carbon dioxide in coal. The modes of carbon dioxide displacement by water injection include water-displacement, gas-dissolution displacement, and gas-diffusion−dissolution displacement. The findings of this study provide novel suggestions for preventing and controlling coal and gas outbursts.

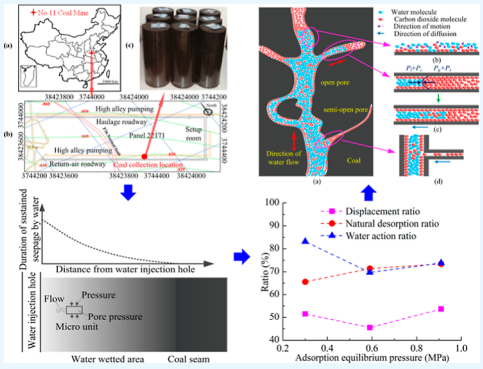

1. INTRODUCTION

Coal and gas outbursts are dynamic disasters caused by gas and broken coal spewing out into a mining space in a short time, which can cause intense damage and seriously threaten safe production in coal mines.[1−3] According to previous reports, coal and gas outbursts have occurred in several major coal-producing countries, including China, Australia, and Canada.[4,5] The volume of gas released during these incidents can reach millions of cubic meters, resulting in a large amount of equipment damage and loss of life. Methane and carbon dioxide are the main gases causing coal and gas outbursts, with carbon dioxide outbursts being the most destructive.[6] Gas extraction is a common measure used in mines to prevent coal and gas outbursts and to enable unconventional natural gas production.[7,8] By arranging boreholes in the coal seam and extracting gas, the gas pressure and the risk of a coal and gas outburst are both reduced.[9−12] However, in some low-permeability coal seams, gas extraction does not easily reach the set targets.[13−15] Some coal mines where the adsorbed gas is carbon dioxide also have encountered this situation, and the efficiency of gas extraction is very low.[16] Exploring new gas extraction modes is one way to solve the poor gas extraction effect.

Long-term research and engineering practice have shown that enhanced coalbed methane recovery can greatly improve gas production. Enhanced coalbed methane recovery has become a trending research topic in gas extraction. The difference in the adsorption capacity of coal to different gases and the injection of gas to change the partial pressure of free gas in the coal seam are mechanisms used to promote the emission of adsorbed gas.[17−19] The injected gases include carbon dioxide, nitrogen, or a mixture of the two.[20,21] According to research, the adsorption of coal to water is stronger than that of coal to methane and carbon dioxide.[22−24] Therefore, theoretically, water can be used to displace methane or carbon dioxide in coal. Researchers have observed that hydraulic measures can increase the gas concentration in roadway airflows.[25−28] A test study on this phenomenon showed that the adsorption of methane on coal surfaces by water replacement is an exothermic process, which indicates that water can replace methane naturally.[29] As more water enters the coal, the replacement amount increases.[30]

Received: November 28, 2023
Revised: February 21, 2024
Accepted: February 27, 2024
Published: March 14, 2024

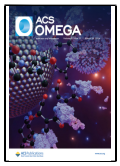

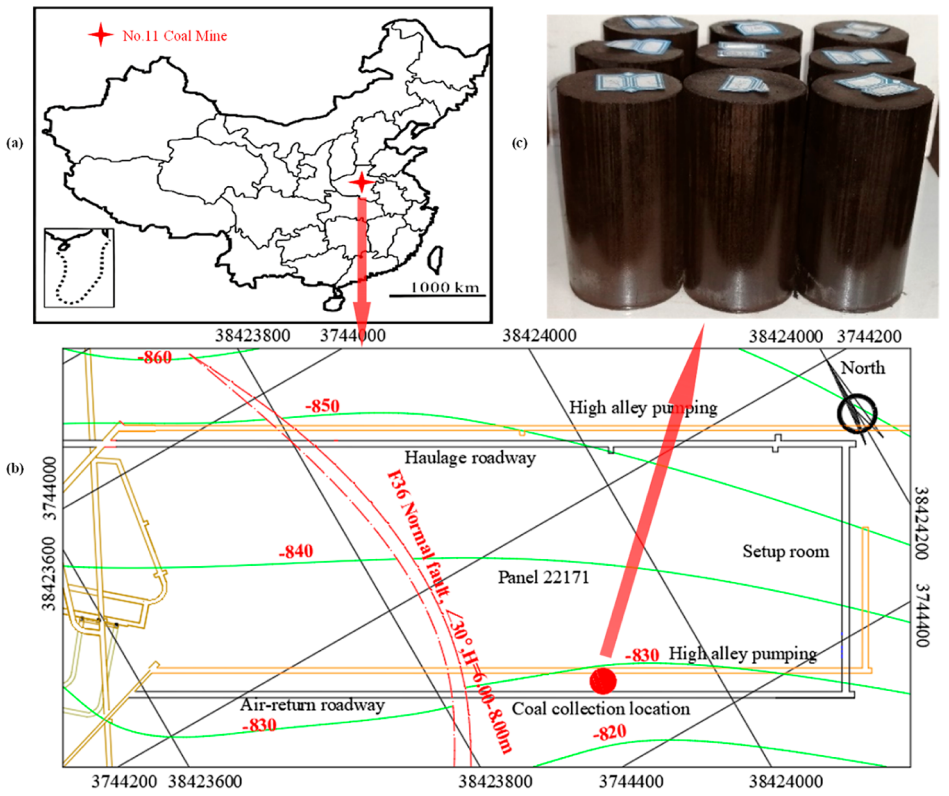

Figure 1. (a) Location of the No. 11 coal mine, (b) coal collection location, and (c) briquette sample.

There is very little research on the displacement of carbon dioxide by water. Only Wang et al. have conducted comparative experiments on the displacement of carbon dioxide by injecting alkaline water and distilled water.[31,32] In addition, all current experiments on the displacement of methane or carbon dioxide by water are carried out with nonflowing water displacement.[30−35] The effects of displacement on free gas or residual gas in the coal sample are analyzed by injecting a quantitative liquid into the coal sample with adsorption equilibrium and monitoring the changes in the gas pressure or changes in the desorption amount after water injection. Displacement under flowing water has not been extensively studied experimentally, and flowing water injection results are more accurate.

In summary, it has been proven that water injection can displace gas adsorbed in coal, but the displacement effect of water on carbon dioxide has not been well revealed, especially the patterns of flowing water injection to displace carbon dioxide gas in coal, which has not been investigated in the current research. Based on this, the experiment of carbon dioxide displacement by water injection under the same water injection pressure and different adsorption equilibrium pressure was carried out through the self-designed experimental device, the patterns of carbon dioxide displacement amount, displacement rate, and displacement ratio were analyzed, and the mode of carbon dioxide displacement by water injection was discussed. The research results provide new suggestions for the management of coalbed methane.

2. MATERIALS AND EXPERIMENTAL PROCEDURES

2.1. Coal Sample Preparation. The No. 11 Coal Mine is a coal and gas outburst mine located in Pingdingshan City, Henan Province. The coal used in this experiment was taken from the 22171 working face, as shown in Figure 1a. Due to the softness at the sampling point, the experiment was carried out with briquettes. The coal was transported to the laboratory and crushed, and pulverized coal with a particle size of 0.38−0.5 mm was screened out by a standard sieve. To obtain the standard coal, a certain quantity of pulverized coal was evenly mixed with water and placed into a coal producing device on a hydraulic press, which was pressed to 100 MPa with the hydraulic press and held for 30 min, as shown in Figure 1b. The samples of briquettes were then kept in a drying oven for 24 h at 60 °C.

2.2. Experimental Device. During coal seam water injection, water in the water injection hole seeps into the coal seams around the borehole under water pressure. As the time of the water injection grows, the water first swiftly flows along the pores and fissures with low resistance before gradually entering with high resistance. As indicated in Figure 2, the closer an area in the coal seam is to the borehole, the longer it will be continuously infiltrated by water, which is the main area where water displacement occurs. Therefore, the displacement should be the process of flowing water displacing gas. In previous experiments of displacing the methane or carbon dioxide adsorbed in coal seams by water, an adsorption tank was filled with a set amount of water, and the displacement effect was studied based on the change in the gas pressure and the desorption volume in the adsorption tank, which is different from the actual situation of coal seam water injection.

Based on the above analysis, an experimental device for two-phase displacement was designed, as shown in Figure 3. The device was composed of a gas adsorption balance system, a vacuum degassing system, a temperature control system, a water injection system, an axial (confining) pressure loading system, and a gas gathering system. The gas (liquid) inlet end of the gas adsorption equilibrium system was connected to a constant-flux pump that could automatically control the water injection

https://doi.org/10.1021/acsomega.3c09502
ACS Omega 2024, 9, 14075−14083

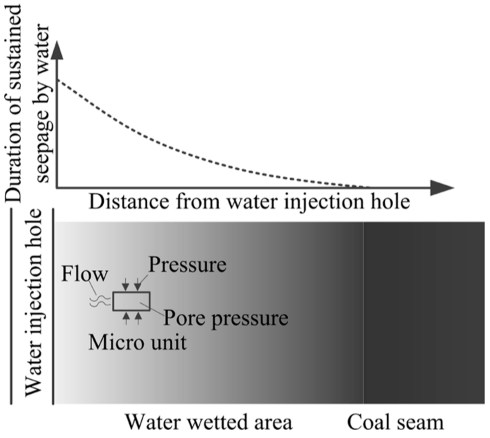

Figure 2. Water seepage law of coal bodies around water injection drilling hole.

pressure and had a maximum water flow of 10 mL/min and a maximum injection pressure of 40 MPa. A pressure control valve with a maximum adjustment pressure of 2.5 MPa was installed on the exhaust (liquid) end. The pressure control valve opens when the pressure at the coal sample discharge end exceeds the set pressure and closes when it is less than the set pressure. The constant-flux pump and pressure control valve controlled the pressure at both ends of the coal sample. The axial pressure loading system and the confining loading system were controlled by the oil and water pressure, respectively. The pumping speed of the vacuum degassing system was 5.9 L/s, and its limit pressure was less than 0.2 Pa. The gas gathering system was equipped with a gas−liquid separation bottle, and the separated gas was collected by discharging a saturated sodium bicarbonate aqueous solution.

2.3. Experimental Procedures. This study conducted two types of experiments: a natural desorption experiment and a water injection displacement experiment. For the same coal sample, a natural desorption experiment was conducted first, followed by inflation adsorption. After adsorption equilibrium was reached, a water injection displacement experiment was conducted. The adsorption equilibrium pressures of the coal sample in the natural desorption experiment and water injection displacement experiment were equal. The natural desorption experiment is a comparative experiment of a water injection displacement experiment to demonstrate the dynamic water injection displacement effect. The experimental scheme is shown in Table 1. The specific experimental process is as follows:

Table 1. Experimental Scheme

number	water injection pressure (MPa)	adsorption equilibrium pressure (MPa)
a	6	0.30
b	6	0.59
c	6	0.91

The coal sample was put into the adsorption tank, and the axial and confining pressures were simultaneously loaded to 8 MPa. Confining pressure was loaded through the water to discharge residual gases from the adsorption tank. The gas tightness was checked, vacuum operation of the system was performed, and then carbon dioxide was injected into the sample for gas adsorption. The adsorption time was 6 h. After adsorption equilibrium, the natural desorption experiment was started and the amount of gas discharged was measured. After the natural desorption experiment, the same coal sample was vacuumed and gas readsorption occurred. When the adsorption equilibrium pressure met these conditions, the opening pressure of the pressure control valve at the discharge end of the experimental device was adjusted to the adsorption equilibrium pressure of the coal sample. The pressure at the water injection port was set at 6 MPa. The constant-flux pump was then activated to initiate the displacement experiment. The stop criterion for both the desorption and displacement experiments was defined as the gas volume at the outlet of the adsorption vessel being less than 0.1 mL/min. The gas volumes were converted to the standard conditions in the experiments. Figure 4 shows the flowchart of the displacement test.

Following the test, the data were further processed to produce various parameters for the analysis of displacements. The calculation equations for each parameter are as follows.

The time displacement rate (TDR) is defined as the ratio of the carbon dioxide displacement volume to the displacement time, as shown in eq 1.

$$v_t = \frac{q_t}{\Delta t} \tag{1}$$

where v_t is the TDR, mL/min; Δt is the displacement time, min; and q_t is the displacement volume of carbon dioxide within the displacement time Δt, mL.

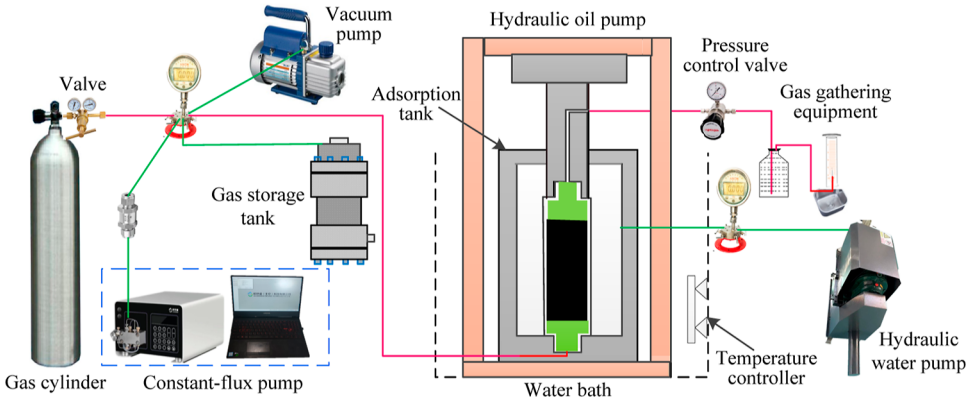

Figure 3. Experimental device.

https://doi.org/10.1021/acsomega.3c09502
ACS Omega 2024, 9, 14075−14083

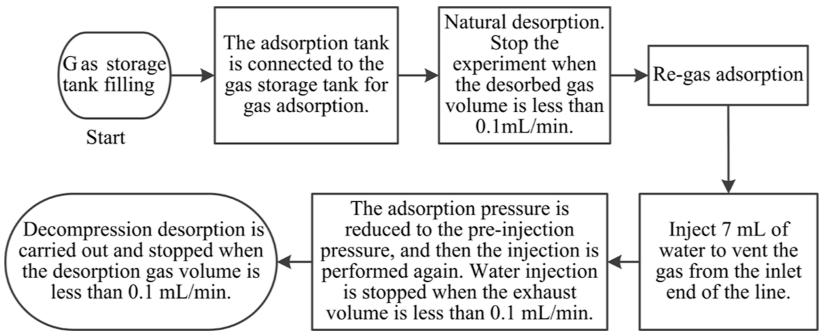

Figure 4. Experimental flowchart.

The water displacement rate (WDR) is defined as the ratio of the carbon dioxide displacement volume to the water injection amount or discharge amount during the displacement time.

$$v_w = \frac{q_t}{q_w} \tag{2}$$

where v_w is the WDR, mL/g; and q_w is the water injection amount or discharge amount during the displacement time Δt, g.

The displacement ratio is defined as the ratio of the carbon dioxide displacement volume to the content of carbon dioxide in a coal sample, as shown in eq 3.

$$\eta_1 = \frac{q_d}{Q} \times 100\% \tag{3}$$

where η_1 is the displacement ratio,%; q_d is the displacement volume, mL; and Q is the content of carbon dioxide in a coal sample, mL.

The water action ratio is defined as the ratio of the sum of the volume of carbon dioxide repelled and dissolved to the content of carbon dioxide in a coal sample. As shown in eq 4,

$$\eta_2 = \frac{q_d + q_s}{Q} \times 100\% \tag{4}$$

where η_2 is the water action ratio,%; and q_s is the volume of carbon dioxide dissolved in water, mL.

The natural desorption ratio is defined as the ratio of the natural desorption volume of carbon dioxide to the content of carbon dioxide in a coal sample. As shown in eq 5,

$$\eta_3 = \frac{q_c}{Q} \times 100\% \tag{5}$$

where η_3 is the natural desorption ratio, %; and q_c is the natural desorption volume of carbon dioxide, mL.

3. RESULTS

3.1. Wettability of Coal Samples. The interior of the coal sample was wetted with water after the test. When the adsorption equilibrium pressures were 0.30, 0.59, and 0.91 MPa, the moisture contents of the coal samples were 11.7, 11.1, and 12.2%, respectively. The water content of the coal samples after the displacement experiment was close to that of the coal samples under natural immersion (11.6% on average), and the coal samples were wetted more sufficiently, which indirectly reflected that displacement occurred in the coal samples.

The moisture content of the coal samples was significantly increased. The water passed through the coal sample, indicating that the test device accurately simulated the process of coal seam water injection and met the test design purpose.

3.2. Amount of Displaced Carbon Dioxide. Figure 5 shows the relationship between the amount of displaced carbon dioxide and the displacement time under different adsorption equilibrium pressures, excluding gas in the water inlet pipe. Figure 6 shows the variation pattern of the natural desorption amount and the amount of displaced carbon dioxide for the same coal sample under the same adsorption equilibrium pressure. It should be noted that the amount of displaced carbon dioxide in Figures 5 and 6 is only the amount of gas collected at the exhaust end and does not take into account the amount of gas dissolved in the discharge water.

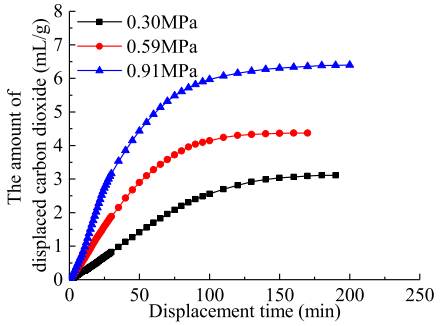

Figure 5. Amount of displaced carbon dioxide under different adsorption equilibrium pressures.

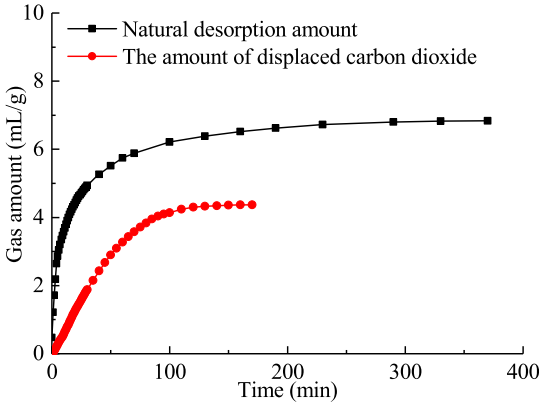

Figure 6. Natural desorption amount and amount of displaced carbon dioxide of coal samples under an adsorption equilibrium pressure of 0.59 MPa.

As shown in Figure 5, the amount of displaced carbon dioxide increased with the displacement time under various adsorption equilibrium pressures. The higher the adsorption equilibrium

https://doi.org/10.1021/acsomega.3c09502
ACS Omega 2024, 9, 14075−14083

pressure, the greater the amount of displaced carbon dioxide and the faster it grew. The speed of increase in the amount of displaced carbon dioxide, on the other hand, gradually decreased and eventually tended to zero. The natural desorption amount of the coal sample was substantially more than the amount of displaced carbon dioxide under the same adsorption equilibrium pressure, as shown in Figure 6. The natural desorption amount increased rapidly and required a long time to desorb, whereas the amount of displaced carbon dioxide increased slowly and required a short time to displace. The curves of the natural desorption amount and the amount of displaced carbon dioxide were divided into three stages: a fast-growth stage, a slow-growth stage, and a stop-growth stage. The growth rate of the natural desorption amount was greater than that of the amount of displaced carbon dioxide in the fast-growth stage, but the duration of the fast-growth stage of the natural desorption amount was shorter than that of the fast-growth stage of the amount of displaced carbon dioxide.

As shown in Figure 5, the trend of the amount of displaced carbon dioxide curve is the same as that of the isothermal adsorption−desorption curve. The characteristics of the isothermal adsorption−desorption curve can be better described by the Langmuir equation[36,37]

$$Q = \frac{abp}{1 + bp} \tag{6}$$

where Q is the gas adsorption amount, mL/g; a is the maximum adsorption amount, mL/g; b is the Langmuir constant, Pa^{-1}; and p is the pore pressure, MPa.

Therefore, an attempt was made to fit the relationship between the amount of displaced carbon dioxide and the displacement time using the structure of the Langmuir equation

$$q = \frac{ABt}{1 + Bt} \tag{7}$$

where q is the amount of displaced carbon dioxide, mL/g; t is the displacement time, min; and A and B are constants.

The fitting results are shown in Table 2. The goodness of fit was close to 1, indicating that eq 7 can effectively describe the relationship between the amount of displaced carbon dioxide and the displacement time. However, parameter A in the equation did not represent the maximum amount of displaced carbon dioxide of the coal samples, which was different from the meaning of parameter A in the Langmuir equation.

Table 2. Relationship between the Amount of Displaced Carbon Dioxide and the Displacement Time

adsorption equilibrium pressure (MPa)	fitting results	constant A	constant B	goodness of fit R^2
0.30	$q = 7.09 \times 0.005t/(1 + 0.005t)$	7.09	0.005	0.99
0.59	$q = 7.24 \times 0.012t/(1 + 0.012t)$	7.24	0.012	0.98
0.91	$q = 9.08 \times 0.017t/(1 + 0.017t)$	9.08	0.017	0.98

3.3. Time and Water Displacement Rate. As shown in Figures 7 and 8, the TDR and WDR change trends were nearly the same and were divided into three stages. (1) The rising stage. In this stage, the injection pressure increased rapidly and tended to the injection pressure after fluctuation, which caused the same change in the seepage pressure difference between the two ends of the coal sample and promoted an increase in gas seepage. Microscopically, the contact area between the water and the coal surface expanded under pressure, leading to an increase in the amount of displaced carbon dioxide. (2) The peak stage. In this stage, the TDR and WDR of coal samples at different adsorption equilibrium pressures fluctuated at higher values, but the duration of the peak stage under different adsorption equilibrium pressures was different. For TDR, when the adsorption equilibrium pressures of the coal samples were 0.30, 0.59, and 0.91 MPa, the duration of the s peak stage was 37, 25, and 10 min, respectively. The higher the adsorption equilibrium pressure, the shorter the duration of the peak stage. The higher the adsorption equilibrium pressure, the higher the pressure at the discharge end, the smaller the pressure drop along the water flow direction, and the higher the pressure at the same position in the coal sample, making it easier for water to enter the small pores. Additionally, the higher the adsorption equilibrium pressure, the greater the solubility of carbon dioxide (the role of solubility is analyzed in detail below), which accelerated the carbon dioxide displacement rate and shortened the duration of the TDR and WDR in the peak stage as the adsorption equilibrium pressure increased. (3) The declining stage. In this stage, the TDR and WDR gradually decreased, and the higher the adsorption equilibrium pressure, the faster decrease in the displacement rate. After the displacement time reached 80 min, the curves of the TDR and WDR under different adsorption equilibrium pressures crossed, and the displacement rate of the coal sample with an adsorption equilibrium pressure of 0.3 MPa was the largest in the subsequent displacement time. The analysis concluded that the displacement rate was determined by the gas content of the

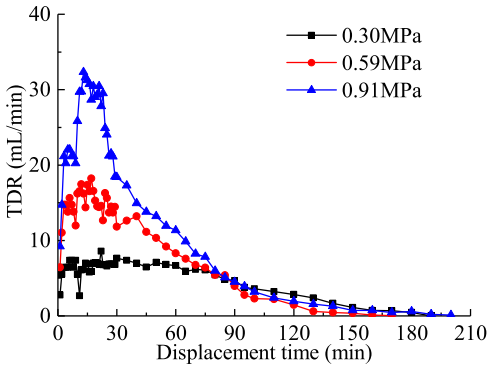

Figure 7. TDR under different adsorption equilibrium pressures.

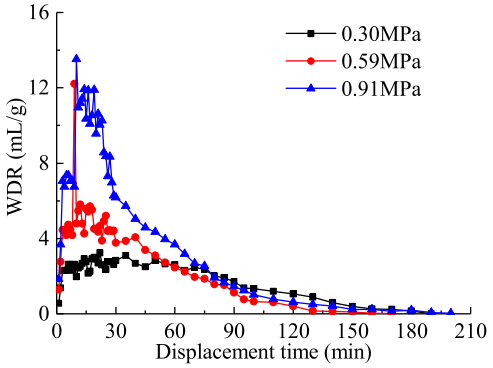

Figure 8. WDR under different adsorption equilibrium pressures.

https://doi.org/10.1021/acsomega.3c09502
ACS Omega 2024, 9, 14075−14083

coal sample in the early displacement stage; that is, the TDR and WDR increased with the adsorption equilibrium pressure. In the later stages of displacement, the difference in the gas content of the coal samples decreased and the effect of the gas content on the TDR and WDR also decreased.

3.4. Displacement Ratio of Carbon Dioxide. Carbon dioxide is soluble in water, and its solubility increases as the temperature and gas pressure increase.[38] According to Aspen Plus software developed by the United States Department of Energy, the solubility of carbon dioxide in water ranges from 0.88 to 33.48 L/L when the temperature is 20 °C and the gas pressure is in the range of 0.1−6 MPa. The small bubble floating phenomenon was observed in the discharged water during the experiment. Therefore, the solubility of carbon dioxide could not be neglected under the test conditions.

During the desorption experiment, due to the high density of carbon dioxide, the gas−liquid separation bottle was filled with carbon dioxide. In the subsequent displacement experiment, the gas separation bottle did not exchange gas with air. Additionally, during the displacement experiment, the gas entering the gas−liquid separation bottle was carbon dioxide. Therefore, in the displacement process, the gas−liquid separation bottle contained only carbon dioxide, and the gas pressure in the bottle was equal to atmospheric pressure. Because there were tiny bubbles in the discharged water, the dissolved volume of carbon dioxide in the discharged water was assumed to have reached a saturated state. Ignoring the volume of carbon dioxide dissolved in water placed in the air under the experimental conditions and the influence of the chemical composition in the coal sample on the solubility of carbon dioxide, the solubility of carbon dioxide in the gas−liquid separation bottle was taken as 0.88 L/L. When the adsorption equilibrium pressures were 0.30, 0.59, and 0.91 MPa, the amount of water discharged at the discharge end was 479.96, 564.05, and 584.76 g excluding the water stored in the coal samples and pipes, respectively, and the dissolved volume of carbon dioxide in the discharged water was approximately 422.36, 496.36, and 514.59 mL.

As demonstrated in Figure 9, at different adsorption equilibrium pressures, the displacement ratio of carbon dioxide

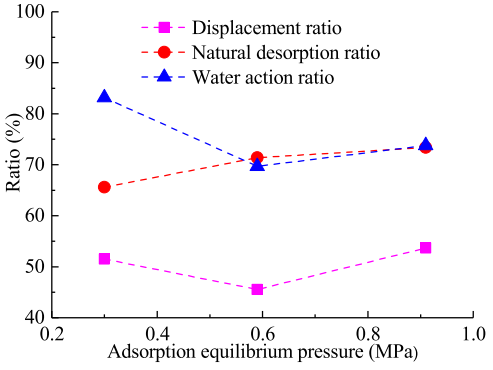

Figure 9. Displacement ratio, natural desorption ratio, and water action ratio under different adsorption equilibrium pressures.

ranged from 45 to 54% with little difference. No consistent relationship was observed between the adsorption equilibrium pressure and the displacement ratio. At different adsorption equilibrium pressures, the displacement ratio was smaller than the natural desorption ratio. But the water action ratio of coal samples with adsorption equilibrium pressures of 0.30 and 0.91 MPa was greater than the natural desorption ratio, whereas the water action ratio of a coal sample with an adsorption equilibrium pressure of 0.59 MPa was slightly lower than the natural desorption ratio. Figure 10 also demonstrates that the

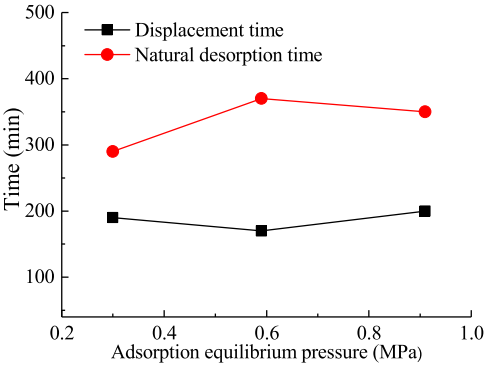

Figure 10. Displacement time and natural desorption time under different adsorption equilibrium pressures.

displacement time was shorter than the natural desorption time. These results show that water effectively displaced carbon dioxide and hastened the desorption of carbon dioxide in the coal samples. Compared with the gas evolution pattern under natural desorption, the coal seam water injection displacement method efficiently displaced a substantial amount of carbon dioxide gas from the coal, resulting in a residual gas content within the coal seam that was lower than the residual gas content under natural desorption conditions, achieving the prevention and control of gas disasters.

4. DISCUSSION

According to the analysis, the amount of displaced carbon dioxide increased with the adsorption equilibrium pressure over the same displacement time. By comparison of the rule of change of expulsion and the rule of change of natural desorption, it was observed that a large amount of carbon dioxide adsorbed gas in coal can be displaced by using flowing water. Using flowing water for displacement clearly hastens the desorption of carbon dioxide in coal by contrasting the displacement pattern with the natural desorption pattern.

According to Zhiguo and Zhaofeng et al., water injection can yield a replacement quantity of approximately 10%, but the water lock effect decreases the overall gas desorption.[39] Zhang et al. discovered that water injection caused the total desorption of coal samples to drop by 26.65% as the water content increased from dry to 1.8%, and they also found that water hindered the pathways for outward gas diffusion in small pores.[40] The common consensus is that adding water to a coal body will both lengthen the time the gas takes to desorb and hinder gas desorption due to the blocking action of water. Without considering the solubility of gas, the experiment still produced the same phenomenon of water obstructing gas in the pores, as illustrated in Figure 11a. However, the experiment used flowing water for uninterrupted injection, and a high fluid pressure was maintained in the coal sample. The carbon dioxide in the coal sample was continuously dissolved in water under the high pressure and later carried out of the coal sample by the flowing water. In the water injection desorption tests, although dissolution occurred during the water injection procedure, the water with dissolved gas remained in the coal body. The dissolved gas was desorbed from the water during the decompression desorption process and was likely adsorbed

https://doi.org/10.1021/acsomega.3c09502
ACS Omega 2024, 9, 14075−14083

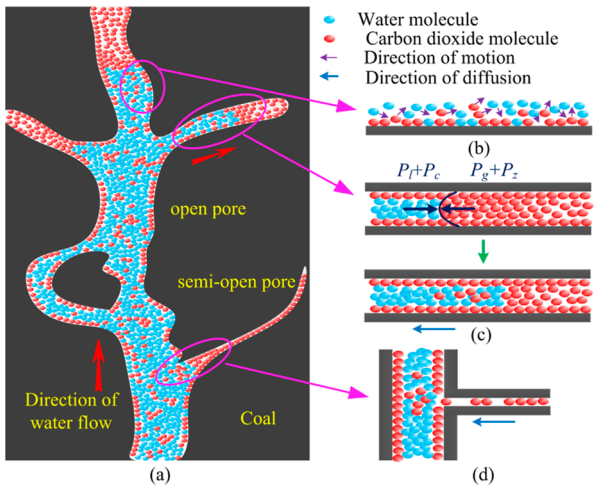

Figure 11. (a) Migration channel in coal, (b) water displacement, (c) gas-dissolution displacement, and (d) gas-diffusion−dissolution displacement.

once more by the coal body. The presence of static water in the pore space, which has a blocking effect, decreased gas desorption.

According to the connectivity results, the pores and fissures in coal can be separated into open pores and fissures and semi-open pores and fissures.[41−43] In the process of water injection, water first flows along the open pores and fissures in the coal, which is called the dominant path. Water continues to pass through the dominant path during the water injection process and then gradually enters the pores and fractures outside the dominant path.[44,45] The ability of water to enter a pore is related to the water injection pressure and pore diameter. The smaller the pore diameter is, the greater the resistance of water entering the pores is.[41] Therefore, water flows along the path with the least resistance first. For the pores and fissures outside the dominant path, at a certain injection pressure and gas pressure (assuming that the gas is insoluble), water struggles to enter the small pores in the coal. However, the small pores contain a large amount of adsorbed gas.[46] These gases cannot be displaced. The blocked gas can be displaced in different modes when the gas can dissolve in water, as shown in Figure 11.

4.1. Water−Gas-Replacement Displacement. The adsorption and desorption of carbon dioxide on the coal surface is a dynamic process.[47] After the carbon dioxide molecules leave the coal surface, the adsorption sites are occupied by water molecules due to the strong adsorption of water by coal. The replaced carbon dioxide molecules are transported outward with flowing water to complete the replacement process, as shown in Figure 11b.

4.2. Gas-Dissolution Displacement. The migration process of water in pores and fractures is simplified to the model shown in Figure 11c. In the dominant path, part of the free gas is driven out of the coal by water. Another part of the free gas is dissolved in water under pressure and discharged with water at the discharge end. After depressurization, part of the gas dissolved in the water is released. Outside the dominant path, in the pore fissures where water can enter, the force equilibrium condition is satisfied at the water−gas interface assuming that the water−gas interface in the pore fissure is in a steady state, as shown in Figure 11c. Thus,[41,48]

$$P_g + P_z = P_c + P_l \tag{8}$$

where P_g is the gas pressure; P_c is the capillary force; P_l is the water pressure, and P_z is the sum of the other forces.

At the water−gas interface in the pore fissure, the free gas on the gas side is continuously dissolved in water. As the gas dissolves, the volume of free gas on the gas side of the water−gas interface decreases. Assuming that the water−gas interface is in a static state, the adsorption equilibrium pressure P_g on the gas side decreases. According to Langmuir adsorption theory, gas desorption occurs on the gas side but the volume of gas desorbed is less than the volume of gas reduced, which prevents the gas pressure on the gas side from returning to the adsorption equilibrium pressure before dissolution. According to eq 8, the water−gas interface cannot be kept in equilibrium, and thus, the water−gas interface will move toward the gas side. The water near the water−gas interface has a large volume of dissolved gas and a high gas concentration in the water, while the gas concentration in the water far from the water−gas interface is low, forming a concentration gradient in the water flow. Under the effect of the concentration gradient, the dissolved gas in water diffuses and migrates from high concentrations to low concentrations.[49,50] The diffusion of dissolved gas will in turn promote the dissolution of gas at the water−gas interface, which forms a cyclic process of "dissolution−desorption−movement−diffusion", and this cyclic process encourages water to enter more pores and fissures. Open pores and fissures form a continuous channel of water flow after the circulation process of "dissolution−desorption−movement−diffusion". In the "dissolution−desorption−movement−diffusion" cycle, the water in the sem-iopen pores and fissures gradually reaches the closed end of the pores and fissures and invades all the pores and fissures. Due to the dissolution of carbon dioxide, the surface area of coal wetted by water gradually expands, so the area where water replaces carbon dioxide also expands, which accelerates the desorption of carbon dioxide from the coal surface. In addition, the dissolved gas also includes the replaced gas.

4.3. Gas-Diffusion−Dissolution Displacement. In the pores where water cannot enter, the pores are small and the gas migrates outward in the form of diffusion. Diffusion conforms to Fick's law of diffusion.[51]

$$J = -D\frac{\partial C}{\partial X} \tag{9}$$

where J is the diffusion velocity, g/(s.cm^2); X is the diffusion path, cm; D is the Fick diffusion coefficient, cm^2/s; and C is the mass concentration of the fluid, g/cm^3.

Water will block the gas in the pores where water cannot enter, but the dissolution of carbon dioxide will occur at the plugging point, resulting in a reduction in the gas concentration on the gas side of the water−gas contact surface and the production of a concentration gradient in the pores, as shown in Figure 11d. The gas diffused from the pores is dissolved at the water−gas interface, resulting in a decrease in the gas concentration on the gas side of the water−gas contact surface, which, in turn, results in a gas concentration gradient in the pores. According to eq 9, the gas diffuses under the effect of the concentration gradient, and the diffusion velocity increases with the gas dissolution velocity. The volume of free gas in the pores decreases, resulting in the desorption of adsorbed gas from the pores. Therefore, in the pores where water does not enter, a cycle of "diffusion−dissolution−desorption" occurs, which accelerates the discharge of gas from the pores. The gas dissolved in water also diffuses, accelerating the displacement of the gas.

https://doi.org/10.1021/acsomega.3c09502
ACS Omega 2024, 9, 14075−14083

Replacement occurs constantly from the time water enters the coal until the experiment ends, and the region where replacement occurs extends as the wetted area of the coal sample grows. However, the volume of replacement diminishes as gas adsorption decreases in the late stages of displacement. This is the reason for the decay of the TDR and WDR. Gas dissolution also occurs after water enters the coal, including the dissolution of free gas, the dissolution of replaced gas, and the dissolution of diffused gas in pores. When the amount of gas produced by displacement is less than the dissolved amount of carbon dioxide in water under the test environment, the discharged water cannot release gas. Then, the gas gathering device will not collect gas, but displacement is still taking place.

5. CONCLUSIONS

(1) The amount of displaced carbon dioxide of coal samples in the same displacement time increases with the adsorption equilibrium pressure, and the growth rate of the amount of displaced carbon dioxide decreases with the displacement time.

(2) The displacement rate of the coal sample increases with the adsorption equilibrium pressure due to the solubility of the gas and the pressure at the discharge end of the adsorption tank, whereas the duration of the coal sample in the peak stage decreases with the adsorption equilibrium pressure.

(3) The displacement ratio of carbon dioxide ranges from 45 to 54% at different adsorption equilibrium pressures, and it is lower than the natural desorption ratio. The water action ratio containing the gas dissolution amount is close to or greater than the natural desorption ratio. The displacement time is shorter than the natural desorption time. These results showed that water effectively displaces carbon dioxide and hastens the desorption of carbon dioxide in coal samples.

(4) There are several different modes in which water injection displaces carbon dioxide, including water displacement, gas-dissolution displacement, and gas-diffusion−dissolution displacement. The combination of the three displacement methods accelerates the displacement rate. The research results provide new methods for the prevention and control of disasters caused by gas.

AUTHOR INFORMATION

Corresponding Authors

Aiwen Wang − *Institute of Disaster Rock Mechanics, Liaoning University, Shenyang 110036, China*; orcid.org/0000-0003-0298-0949; Email: waw_lgd@126.com

Helian Shen − *Institute of Disaster Rock Mechanics, Liaoning University, Shenyang 110036, China*; Email: 2867544963@qq.com

Authors

Tianwei Shi − *Institute of Disaster Rock Mechanics, Liaoning University, Shenyang 110036, China*

Yishan Pan − *Institute of Disaster Rock Mechanics, Liaoning University, Shenyang 110036, China*

Lianpeng Dai − *Institute of Disaster Rock Mechanics, Liaoning University, Shenyang 110036, China*

Complete contact information is available at: https://pubs.acs.org/10.1021/acsomega.3c09502

Author Contributions

T.S.: writing—original draft and visualization. Y.P.: conceptualization, supervision, and funding acquisition. A.W.: supervision and funding acquisition. L.D.: writing—review and editing and experiment. H.S.: writing—review and editing. All authors reviewed the manuscript.

Funding

This study was funded by the General Program of the National Natural Science Foundation of China (no. 51974150) and the Department of Science and Technology of Liaoning Province (2023-BS-083). The authors also thank anonymous colleagues for their kind efforts and valuable comments in improving this work.

Notes

The authors declare no competing financial interest.

REFERENCES

(1) Beamish, B. B.; Crosdale, P. J. Instantaneous outbursts in underground coal mines: an overview and association with coal type. *Int. J. Coal Geol.* **1998**, *35*, 27−55.

(2) Sobczyk, J. A comparison of the influence of adsorbed gases on gas stresses leading to coal and gas outburst. *Fuel* **2014**, *115*, 288−294.

(3) Si, J.; Li, L.; Cheng, J.; Wang, Y.; Hu, W.; Li, T.; Li, Z. Characteristics of Airflow Reversal of Excavation Roadway after a Coal and Gas Outburst Accident. *Energies* **2021**, *14*, 3645.

(4) Cao, Y.; He, D.; Glick, D. C. Coal and gas outbursts in footwalls of reverse faults. *Int. J. Coal Geol.* **2001**, *48*, 47−63.

(5) Xue, S.; Zheng, C.; Jiang, B.; Zheng, X. Effective potential energy associated with coal and gas outburst during underground coal mining: case studies for mining safety. *Arabian J. Geosci.* **2021**, *14*, 1065.

(6) Wu, D.; Zhao, Y.; Cheng, Y.; An, F. ΔP index with different gas compositions for instantaneous outburst prediction in coal mines. *Min. Sci. Technol.* **2010**, *20*, 723−726.

(7) Li, Y.; Pan, S.; Ning, S.; Shao, L.; Jing, Z.; Wang, Z. Coal measure metallogeny: Metallogenic system and implication for resource and environment. *Sci. China: Earth Sci.* **2022**, *65*, 1211−1228.

(8) Li, Y.; Yang, J.; Pan, Z.; Meng, S.; Wang, K.; Niu, X. Unconventional natural gas accumulations in stacked deposits: a discussion of upper paleozoic coal-bearing strata in the east margin of the ordos basin, China. *Acta Geol. Sin.* **2019**, *93*, 111−129.

(9) Cao, W.; Shi, J.; Durucan, S.; Si, G.; Korre, A. Gas-driven rapid fracture propagation under unloading conditions in coal and gas outbursts. *Int. J. Rock Mech. Min. Sci.* **2020**, *130*, 104325.

(10) Yuan, L. Theory and practice of integrated coal production and gas extraction. *Int. J. Coal Sci. Technol.* **2015**, *2*, 3−11.

(11) Ibrahim, A. F.; Nasr-El-Din, H. A. A comprehensive model to history match and predict gas/water production from coal seams. *Int. J. Coal Geol.* **2015**, *146*, 79−90.

(12) Zhang, H.; Xu, L.; Yang, M.; Deng, C.; Cheng, Y. Pressure Relief Mechanism and Gas Extraction Method during the Mining of the Steep and Extra-Thick Coal Seam: A Case Study in the Yaojie No. 3 Coal Mine. *Energies* **2022**, *15*, 3792.

(13) Gao, Y.; Lin, B.; Yang, W.; Li, Z.; Pang, Y.; Li, H. Drilling large diameter cross-measure boreholes to improve gas drainage in highly gassy soft coal seams. *J. Nat. Gas Sci. Eng.* **2015**, *26*, 193−204.

(14) Si, G.; Durucan, S.; Shi, J.; Korre, A.; Cao, W. Parametric analysis of slotting operation induced failure zones to stimulate low permeability coal seams. *Rock Mech. Rock Eng.* **2019**, *52*, 163−182.

(15) Liu, Y.; Li, H.; Shen, H.; Deng, Y.; Liu, X. Study on the development law of self-oscillating pulsed SC-CO2 jet vortex structure and its effect on frequency. *Geomech. Geophys. Geo-Energy Geo-Resour.* **2023**, *9*, 94.

(16) Aziz, N.; Black, D.; Ren, T. Keynote paper mine gas drainage and outburst control in Australian underground coal mines. *Procedia Eng.* **2011**, *26*, 84−92.

(17) Li, Y.; Zhang, C.; Tang, D.; Gan, Q.; Niu, X.; Wang, K.; Shen, R. Coal pore size distributions controlled by the coalification process: An

https://doi.org/10.1021/acsomega.3c09502
ACS Omega 2024, 9, 14075−14083

experimental study of coals from the Junggar, Ordos and Qinshui basins in China. *Fuel* **2017**, *206*, 352−363.
(18) Li, Y.; Yang, J.; Pan, Z.; Tong, W. Nanoscale pore structure and mechanical property analysis of coal: an insight combining AFM and SEM images. *Fuel* **2020**, *260*, 116352.
(19) Li, Y.; Wang, Y.; Wang, J.; Pan, Z. Variation in permeability during CO2-CH4 displacement in coal seams: part 1-experimental insights. *Fuel* **2020**, *263*, 116666.
(20) Zhang, L.; Li, J.; Xue, J.; Zhang, C.; Fang, X. Experimental studies on the changing characteristics of the gas flow capacity on bituminous coal in CO_2-ECBM and N_2-ECBM. *Fuel* **2021**, *291*, 120115.
(21) Pini, R.; Ottiger, S.; Storti, G.; Mazzotti, M. Pure and competitive adsorption of CO_2, CH_4 and N_2 on coal for ECBM. *Energy Procedia* **2009**, *1*, 1705−1710.
(22) Zhu, H.; Zhang, Y.; Qu, B.; Liao, Q.; Wang, H.; Gao, R. Thermodynamic characteristics of methane adsorption about coking coal molecular with different sulfur components: considering the influence of moisture contents. *J. Nat. Gas Sci. Eng.* **2021**, *94*, 104053.
(23) Chen, M.; Cheng, Y.; Li, H.; Wang, L.; Jin, K.; Dong, J. Impact of inherent moisture on the methane adsorption characteristics of coals with various degrees of metamorphism. *J. Nat. Gas Sci. Eng.* **2018**, *55*, 312−320.
(24) Zhou, W.; Wang, H.; Zhang, Z.; Chen, H.; Liu, X. Molecular simulation of CO_2/CH_4/H_2O competitive adsorption and diffusion in brown coal. *RSC Adv.* **2019**, *9*, 3004−3011.
(25) Huang, B.; Lu, W. A fluid-solid coupling mathematical model of methane driven by water in porous coal. *Geofluids* **2018**, *2018*, 1−17.
(26) Huang, B.; Cheng, Q.; Chen, S. The verification of displacement methane effect caused by hydraulic fracturing in gassy coal seams. *Arabian J. Geosci.* **2018**, *11*, 638.
(27) Lu, W.; Huang, B. Numerical simulation of migration characteristics of the two-phase interface in water-gas displacement. *Energy Explor. Exploit.* **2018**, *36*, 246−264.
(28) Huang, B.; Cheng, Q.; Chen, S. Phenomenon of methane driven caused by hydraulic fracturing in methane-bearing coal seams. *Int. J. Min. Sci. Technol.* **2016**, *26*, 919−927.
(29) Yang, W.; Lu, C.; Si, G.; Lin, B.; Jiao, X. Coal and gas outburst control using uniform hydraulic fracturing by destress blasting and water-driven gas release. *J. Nat. Gas Sci. Eng.* **2020**, *79*, 103360.
(30) Wu, J.; Yu, J.; Wang, Z.; Fu, X.; Su, W. Experimental investigation on spontaneous imbibition of water in coal: implications for methane desorption and diffusion. *Fuel* **2018**, *231*, 427−437.
(31) Wang, M.; Yang, Y.; Miao, G.; Zheng, K.; Zhou, X. An experimental study on coal damage caused by two-phase displacement of CO_2-alkaline solution. *J. Nat. Gas Sci. Eng.* **2021**, *93*, 104034.
(32) Yang, Y.; Si, L.; Li, Z.; Li, J.; Li, Z. Experimental study on effect of CO_2-alkaline water two-phase gas displacement and coal wetting. *Energy Fuels* **2017**, *31*, 14374−14384.
(33) Ni, G.; Lin, B.; Zhai, C.; Li, Q.; Peng, S.; Li, X. Kinetic characteristics of coal gas desorption based on the pulsating injection. *Int. J. Min. Sci. Technol.* **2014**, *24*, 631−636.
(34) Hu, Y.-L.; Wu, X. Research on coalbed methane reservoir water blocking damage mechanism and anti-water blocking. *J. China Coal Soc.* **2014**, *39*, 1107−1111.
(35) Chen, X.; Li, L.; Cheng, Y.; Qi, L. Experimental study of the influences of water injections on CBM exploitation. *Energy Sources, Part A* **2022**, *44*, 1033−1044.
(36) Dutta, P.; Harpalani, S.; Prusty, B. Modeling of CO_2 sorption on coal. *Fuel* **2008**, *87*, 2023−2036.
(37) Ye, J.; Tao, S.; Zhao, S.; Li, S.; Chen, S.; Cui, Y. Characteristics of methane adsorption/desorption heat and energy with respect to coal rank. *J. Nat. Gas Sci. Eng.* **2022**, *99*, 104445.
(38) Dodds, W.; Stutzman, L.; Sollami, B. Carbon dioxide solubility in water. *Ind. Eng. Chem. Chem. Eng. Data Ser.* **1956**, *1*, 92−95.
(39) Zhiguo, X.; Zhaofeng, W. Experimental study on inhibitory effect of gas desorption by injecting water into coal-sample. *Procedia Eng.* **2011**, *26*, 1287−1295.
(40) Zhang, K.; Cheng, Y.; Wang, L.; Dong, J.; Hao, C.; Jiang, J. Pore morphology characterization and its effect on methane desorption in water-containing coal: An exploratory study on the mechanism of gas migration in water-injected coal seam. *J. Nat. Gas Sci. Eng.* **2020**, *75*, 103152.
(41) Lu, W.; Huang, B.; Zhao, X. A review of recent research and development of the effect of hydraulic fracturing on gas adsorption and desorption in coal seams. *Adsorpt. Sci. Technol.* **2019**, *37*, 509−529.
(42) Zhang, Z.; Qin, Y.; Yi, T.; You, Z.; Yang, Z. Pore structure characteristics of coal and their geological controlling factors in Eastern Yunnan and Western Guizhou, China. *ACS Omega* **2020**, *5*, 19565−19578.
(43) Liu, S.; Li, X.; Wang, D.; Zhang, D. Investigations on the mechanism of the microstructural evolution of different coal ranks under liquid nitrogen cold soaking. *Energy Sources, Part A* **2020**, 1−17.
(44) Liu, Z.; Yang, H.; Wang, W.; Cheng, W.; Xin, L. Experimental study on the pore structure fractals and seepage characteristics of a coal sample around a borehole in coal seam water infusion. *Transp. Porous Media* **2018**, *125*, 289−309.
(45) Pan, Y.-S.; Tang, J.; Li, C. NMRI test on two-phase transport of gas-water in coal seam. *Chin. J. Geophys.* **2008**, *51*, 1620−1626.
(46) Zou, Q.; Lin, B.; Liang, J.; Liu, T.; Zhou, Y.; Yan, F.; Zhu, C. Variation in the pore structure of coal after hydraulic slotting and gas drainage. *Adsorpt. Sci. Technol.* **2014**, *32*, 647−666.
(47) Tang, X.; Ripepi, N.; Gilliland, E. Isothermal adsorption kinetics properties of carbon dioxide in crushed coal. *Greenhouse Gases: Sci. Technol.* **2016**, *6*, 260−274.
(48) Zhang, J.; Wang, R.; Yang, F.; Lei, W.; Feng, B.; Zheng, C.; Zhang, J.; Miao, Z. Discussion on the mechanism of coal and gas outburst prevention and control by the coal seam water injection. *IOP Conf. Ser.: Earth Environ. Sci.* **2019**, *252*, 052090.
(49) Gholami, Y.; Azin, R.; Fatehi, R.; Osfouri, S. Suggesting a numerical pressure-decay method for determining CO_2 diffusion coefficient in water. *J. Mol. Liq.* **2015**, *211*, 31−39.
(50) Orgogozo, L.; Golfier, F.; Buès, M. A.; Quintard, M.; Koné, T. A dual-porosity theory for solute transport in biofilm-coated porous media. *Adv. Water Resour.* **2013**, *62*, 266−279.
(51) Milligen, B. P. v.; Bons, P.; Carreras, B. A.; Sanchez, R. On the applicability of Fick's law to diffusion in inhomogeneous systems. *Eur. J. Phys.* **2005**, *26*, 913−925.

https://doi.org/10.1021/acsomega.3c09502
ACS Omega 2024, 9, 14075−14083